Journal of Statistical Physics, Vol. 61, Nos. 1/2, 1990

Theory on Morphological Instability in Driven Systems

Kwan-tai Leung[1]

Received December 19, 1989; final April 2, 1990

Motivated by recent findings from simulation of a driven lattice gas under shifted periodic boundary conditions, we study within the context of a continuum model the interfacial stability of driven diffusive systems. In this model, an external driving field maintains the system away from equilibrium. Well below criticality, steady-state solutions of the associated bulk kinetic equation are obtained. Our results successfully account for the novel features found in simulation. In particular, the solution describing a pair of interfaces tilted with respect to the driving field under periodic boundary conditions shows a tilt-dependent bulk density (and internal energy), and boundary layers near one of the interfaces. Focusing on the interface dynamics, one finds that such an interface exhibits a characteristic Mullins–Sekerka instability. This is argued to be responsible for the onset of the single- to multistrip transformation observed in simulation.

KEY WORDS: Nonequilibrium steady state; interface; instability.

1. INTRODUCTION

The study of nonequilibrium systems has a long history. One of the prototype systems pursued in recent years is a stochastic model of a lattice gas of particles driven by an external field E.[1] The effect of E on the hopping dynamics is analogous to that of a uniform electric field acting on charged particles. This systems exhibits a bulk phase transition akin to the phase separation in equilibrium binary systems. Recent studies,[2–4] focused on the interfaces, revealed a multitude of interesting phenomena, some of which still defy complete theoretical explanation. Among them include the suppression of interfacial roughening in two dimensions[3] and the behavior

[1] Department of Physics, Virginia Polytechnic Institute and State University, Blacksburg, Virginia 24061.

0022-4715/90/1000-0345$06.00/0

induced by imposing shifted periodic boundary conditions (SPBC) (also known as screw boundary conditions).[4]

Under SPBC at low temperature, the system phase separates into a particle-rich and a particle-poor phase separated by two interfaces which are tilted by a certain angle (as determined by the amount of shift) against the field. The original motivation of such a study is to establish a connection of the suppression of roughness to the nonanalytic property of the interfacial energy. Unexpected additional results emerged, however, that place a much more important role than in equilibrium on the boundary conditions in determining even bulk properties. Without the field, the system becomes in equilibrium; the influence of the boundary conditions on the bulk is totally absent. To summarize, the novel features include the following[4]: (1) There are two distinct interfaces (see Fig. 4 for an illustration), the "leading" edge (away from which particles are driven) appears rough, while the "trailing" one (toward which particles are driven) appears smooth. (2) The *bulk* energy has nonanalytic dependence on the shift. (3) Boundary layers exist near the trailing edge. (4) At a certain angle of tilt (depending on system size), the system undergoes a single- to multistrip "splitting" transition, and subsequently a series of "merging" transitions on further shifting. In ref. 4, we offered qualitative arguments in favor of these observations based on the absorbing and evaporating nature of the trailing and leading edge, respectively. However, satisfactory quantitative understanding is still lacking.

In a different but complementary approach to simulation, a coarse-grained continuum model adopted from field theory has provided us with insight into some of the unusual bulk[5,6] and interfacial properties[2] of these driven diffusive systems. In this paper, we propose, based on such a continuum model, that the above phenomena can be explained within a similar framework used in other theoretical analyses of interfacial stability. Prominent examples of such analyses are dendritic crystal growth[7] and the Saffman–Taylor problem,[8] which involves two-fluid displacement in a confined geometry. We will show that a close analogy to these problems of pattern formation is not only exhibited in the resemblances of the evolution of the objects (clusters) generated, but also in similar mathematical structure of the equations.

Section 2 is devoted to our continuum model and its steady-state solutions of tilted planar interfaces under various boundary conditions. Section 3 contains a linear stability analysis appropriate to the tilted interfaces. In Section 4, comparisons with simulation results are made. Finally, a discussion of the physical content of Section 3 and the conclusion of this paper are presented in Section 5.

2. STEADY STATE SOLUTIONS

Our starting point of the theoretical description of the interfacial instability is a Langevin equation of the bulk density. Such an equation has been used in the renormalization group analysis of the critical bulk properties,[6] as well as in previous interfacial studies.[2] It is based on the kinetic equation of the model B,[9] supplemented by a term modeling the driven current: $J_E = \sigma(\phi)\, E$. After expanding the conductivity $\sigma(\phi)$ about $\phi = 0$ up to quadratic term and performing a Galilean transformation to eliminate the linear term in ϕ, we get[5,6]

$$\begin{aligned}\frac{\partial \phi}{\partial t} &= -\nabla \cdot J_{\text{tot}} \\ &= \frac{1}{2}\lambda E \partial_{\parallel} \phi^2 + \lambda \nabla^2 \frac{\delta \mathscr{H}}{\delta \phi} + \eta \\ &= \frac{1}{2}\lambda E \partial_{\parallel} \phi^2 + \lambda \nabla^2 \left[(r - \nabla^2)\, \phi + \frac{1}{6} g \phi^3 \right] + \eta \end{aligned} \tag{2.1}$$

where $\mathscr{H}$ is the usual ϕ^4 "Hamiltonian":

$$\mathscr{H} = \int d^d x \left[\frac{1}{2} (\nabla \phi)^2 + \frac{1}{2} r \phi^2 + \frac{1}{4!} g \phi^4 \right] \tag{2.2}$$

Here $\phi(x)$ is the magnetization density, related to the particle density $n(x)$ by $\phi = 2n - 1$; λ is the transport coefficient; the symbol $\partial_{\parallel}$ denotes derivative with respect to the spatial coordinate parallel to E; and η is a Gaussian white noise. Although E in general generates spatial anisotropies in the parameters coupled to the derivatives, they will be neglected hereafter in order to simplify our analysis, as they will not change the essential qualitative features of the solutions. In what follows we will only consider temperature well below T_c, so that $r < 0$. In such a regime, the amplitude of thermal fluctuations is negligibly small, enabling us to consider just the deterministic equation (i.e., the equation without η). In general, the solution of such an equation is still very complicated. Since we are only interested in the steady-state solutions, some general properties can be obtained from simple analysis. From now on we will focus on two dimensions.

Since the system phase separates below T_c, we seek a steady-state solution with *planar* interface(s) separating the two bulk phases. Let θ be the orientation of the interface(s) relative to E, which points along the $+y$ direction. The above equation can be cast into a simpler form by defining dimensionless variables: $\psi(u, v, \tau) = \phi(x, y, t)/\phi_{\text{eq}}$, $u = (-x \cos\theta + y \sin\theta)/a$, $v = (x \sin\theta + y \cos\theta)/a$, and $\tau = a^{-4} \lambda t$ are the

respective dimensionless density function, dimensionless distances measured from and along the interface, and the dimensionless time. The scales are set by the usual model-B equilibrium magnetization and interfacial width: $\phi_{eq}^2 = -6r/g$, $a = 1/(-r)^{1/2}$. With this rescaling, the only parameter left is

$$\varepsilon = \tfrac{1}{2} E \phi_{eq} a^3 \sin\theta \tag{2.3}$$

By translational invariance along the interfaces, the steady-state solution depends only on u. It satisfies

$$\varepsilon\psi^2 - \psi' - \psi''' + 3\psi^2\psi' = J \tag{2.4}$$

where the integration constant J contributes negatively to the current normal to the interfaces. Now we discuss some general features of the steady-state solution. Without loss of generality, we consider $\varepsilon > 0$.

Reduction of Order. Consider solutions which satisfy $\psi(u=0)=0$; i.e., having the line $u=0$ as the center of one of the interfaces. Integrating (2.4) once, we obtain a second-order integral-differential equation:

$$\psi + \psi'' - \psi^3 = \int_0^u du(\varepsilon\psi^2 - J) \tag{2.5}$$

Multiplying by ψ' and integrating by part reduces (2.5) to a first-order equation:

$$\tfrac{1}{2}\psi^2 + \tfrac{1}{2}\psi'^2 - \tfrac{1}{4}\psi^4 = \tfrac{1}{2}\psi'(0)^2 + \int_0^u du'[\psi(u) - \psi(u')][\varepsilon\psi(u')^2 - J] \tag{2.6}$$

Now consider solutions to (2.4) corresponding to phase-separated states in a system of linear dimension L.

Single Interface for $L = \infty$. For an infinite system, the solutions describing a single planar interface, separating two bulk phases at uniform bulk density $\psi(\pm\infty) = \pm\psi_\infty$, satisfy $J = \varepsilon\psi_\infty^2$. We assume that $\psi(u)$ is monotonic, since there is no physical reason or numerical evidence for ψ to be otherwise. It follows from (2.5) that $\psi_\infty^2 < 1$ or > 1 for $\psi_\infty < 0$ or > 0, respectively. This asymmetry, as induced by E, is important to the stability analysis in the next section. Notice that $\psi(u)$ becomes a simple tanh with $\psi_\infty^2 = 1$ for $\varepsilon = 0$.

For $L = \infty$, the tanh is also a solution for $\varepsilon \neq 0$:

$$\psi(u) = \psi_\infty \tanh(u/\xi) \tag{2.7a}$$

with

$$\psi_\infty^2 = \begin{cases} 1+\sqrt{2}\,\varepsilon \equiv \psi_t, & \psi(\infty) > 0 \\ 1-\sqrt{2}\,\varepsilon \equiv \psi_l, & \psi(\infty) < 0 \end{cases} \tag{2.7b}$$

for "trailing" or "leading" interface, respectively; $\xi^{-2} = \frac{1}{2}\psi_\infty^2$, $J = \varepsilon\psi_\infty^2$, and $\psi'(0) = \psi_\infty^2/\sqrt{2}$. Although it is not necessarily the only solution in the whole functional space, the tanh is obviously important at least for small ε: one naturally arrives at these solutions in a perturbation expansion in small ε.

PBC Solution for Finite L. Periodic boundary condition (PBC) is physically relevant to either real systems or computer simulations. It is probably the only boundary condition conceivable to give rise to nonzero current along E. It is also of mathematical interest as to what solution the system would pick in the presence of an asymmetry of the two interfaces, for now we must have two coexisting, parallel interfaces in the system. Let us look for solutions such that $\psi > 0$ for $0 < u < L/2$, and $\psi < 0$ for $L/2 < u < L$.

Due to nonlinearities, we resort to numerical methods[10] in finding the solutions. Solutions were obtained for both weak and strong field strength, $\varepsilon = 0.2$, 0.4, and 0.6, starting from small to large period L, until a plateau in the bulk density ψ_B was observed. Some typical solutions are presented in Fig. 1. We observed some important features:

(a) There exists a hump near the trailing interface, which has a peak value lying between the bulk densities ψ_l and ψ_t of the tanh profiles. The same is true for the slope $\psi'(0)$.

(b) The extent of the hump is independent of L for large enough L. It is therefore a *boundary layer* associated with the trailing interface.

(c) There is oscillation in the tail of the hump for sufficiently large ε.

(d) No bounded solution was found for $J < \varepsilon\psi_l^2$. Solutions exist only for $J > \varepsilon\psi_l^2$; L increases with decreasing $J - \varepsilon\psi_l^2$.

(e) At the leading interface, the profile approaches the tanh solution (2.7) in the limit of $L \to \infty$, as $J \to \varepsilon\psi_l^2$ from above.

Additional insight can be obtained from (2.4) and (2.5). First, away from the interfaces, a linearization of (2.4) predicts an exponential decay of $\psi(u)$ to a constant ψ_B, in the form of $e^{\lambda u}$ with λ determined by

$$\lambda^3 + (1 - 3\psi_B^2)\,\lambda - 2\varepsilon\psi_B = 0 \tag{2.8}$$

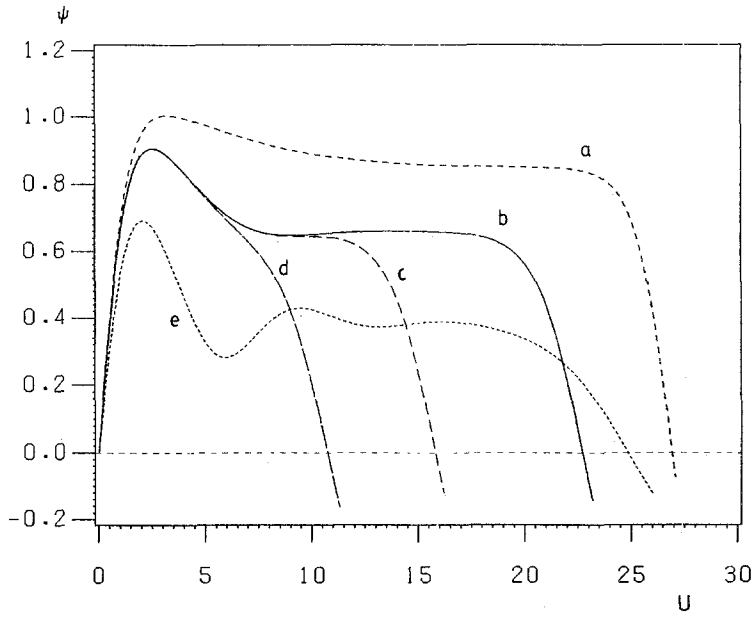

Fig. 1. Plots of some typical numerical solutions of (2.4). (a) $\varepsilon = 0.2$, $\varepsilon\psi_I^2 = 0.1434$, $J = 0.1436$, $L/2 = 27$; (b) $\varepsilon = 0.4$, $\varepsilon\psi_I^2 = 0.1737$, $J = 0.1738$, $L/2 = 22.7$; (c) $\varepsilon = 0.4$, $J = 0.1739$, $L/2 = 15.8$; (d) $\varepsilon = 0.4$, $J = 0.1746$, $L/2 = 10.7$; (e) $\varepsilon = 0.6$, $\varepsilon\psi_I^2 = 0.0909$, $J = 0.091$, $L/2 = 24.8$. Notice the boundary layers near the trailing interface. Driving field E points to the right.

This equation has one positive real root (λ_1), and two others (λ_2, λ_3) with negative real parts. Substituting ψ_I for ψ_B, we find $\lambda_2 = \lambda_3^*$ for $\varepsilon > \varepsilon_c = 1/3\sqrt{2}$, and λ_2 and λ_3 are real otherwise. λ_1 accounts for the exponential deviation from ψ_B at the leading interface; whereas λ_2 and λ_3 account for the decay away from the hump, with oscillation for $\varepsilon > \varepsilon_c$. For $\varepsilon \ll 1$, one of the negative roots goes as $-\varepsilon$, yielding a long tail. This exponential decay away from the trailing interface is consistent with the hump being L independent. For the values of ε used in the numerical solutions, we find, denoting $\lambda_2 = \lambda_R + i\lambda_I$ in the case of complex roots: (a) $\varepsilon = 0.2$: $\lambda_2 = -0.3236$, $\lambda_3 = -0.8740$; (b) $\varepsilon = 0.4$: $\lambda_R = -0.4660$, $\lambda_I = 0.5904$; (c) $\varepsilon = 0.6$: $\lambda_R = -0.2752$, $\lambda_I = 0.8791$. These agree with the estimates from Fig. 1. Judging from the distortion of the profile compared to $\varepsilon = 0$, $\varepsilon = 0.6$ is regarded as a strong field.

Furthermore, we may argue on the basis of (2.4) that the boundary layer appears only near the trailing edge. To see this, we recall that the total current along E is given by $J_{\text{tot}} = J_0 - J$, with $J_0 = \sigma(\phi = 0)\, E$ the constant term eliminated upon taking the derivative in (2.1). At the tail of the hump, we may make the approximation $J \approx \varepsilon\psi^2 + (3\psi^2 - 1)\,\psi'$ (see Fig. 2),

where the second term is identified as the diffusive current. For the sake of argument, let us assume that ε is small (more precisely, $\varepsilon < 2\varepsilon_c$), so that we take $3\psi^2 - 1 > 0$. In the steady state, the current must be uniform at $J_{\text{tot}} = J_0 - \varepsilon\psi_B^2$, i.e., the value deep in the bulk. It is clear, then, that if the hump sits near the leading edge, both terms in J would contribute to a reduction from those at ψ_B, implying that a boundary layer near the leading edge is inconsistent with the steady-state condition of a uniform J_{tot} everywhere. In contrast, it is consistent to have a boundary layer near the trailing edge.

Next, assuming the existence of a boundary layer near the trailing interface, we can derive some inequalities on ψ_B. We arbitrarily pick a point u_B in the bulk, i.e., $\psi(u_B) = \psi_B$, as the upper integration limit in (2.5):

$$\psi_B(1 - \psi_B^2) = \varepsilon \int_0^{u_B} du[\psi(u)^2 - \psi_B^2] \tag{2.9}$$

Since we assume that the hump is situated near $u = 0$, $\int_{u_B}^{L/2} du[\psi(u)^2 - \psi_B^2]$ is negative. Subtracting (2.9) from $\int_0^{L/2} du[\psi(u)^2 - \psi_B^2] = 0$ then yields $1 - \psi_B^2 > 0$. We therefore arrive at the following:

$$0 < \psi_l \leqslant \psi_B < 1 < \psi_t \tag{2.10}$$

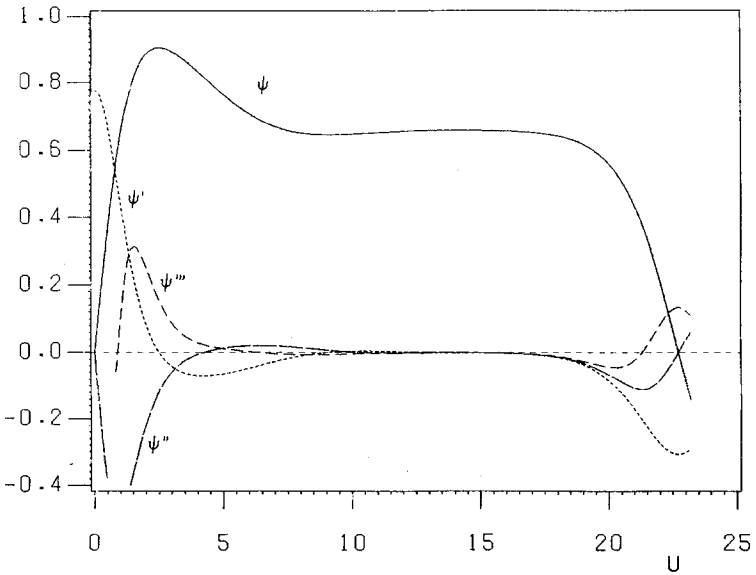

Fig. 2. Plots of ψ and its derivatives for the case of Fig. 1b, showing the region of validity of (3.1), in which ψ''' may be neglected compared to ψ' away from the hump and the leading interface.

It is a numerical finding that the only possible value of ψ_B is ψ_l. The question remains open as to why, physically, the leading edge value of infinite-L solution is selected under PBC. Note that $J_{\text{tot}}(\psi_t) < J_{\text{tot}}(\psi_l)$, implying that the steady state favors a larger current. Whether this has any connection with the principle of maximum entropy production deserves further investigation. In connection with simulation, since the bulk density equals the trailing edge value ψ_l, it is easy to see from (2.7b) and (2.3) that the bulk density, hence the bulk energy, acquires nonanalytic dependence of the angle of tilt in the form of $|\theta|$ as $\theta \to 0$, consistent with our previous finding.[4]

Before closing this section, a few remarks are in order:

1. Given the PBC solution, suppose we take the limit $L \to \infty$. We would then end up with a solution of one trailing interface with humps on both sides, while $\psi(u \to \pm\infty) \to \pm\psi_B$. Now we regard J in (2.4) as a function of L and ε. We take the limit $L \to \infty$ first, and we try to find the humps perturbatively by expanding everything about $\varepsilon = 0$. This instead yields the tanh solution for $L = \infty$ mentioned above. This means that under PBC the two limits $\lim_{L\to\infty}$ and $\lim_{\varepsilon\to 0}$ approach the $\varepsilon = 0$, $L = \infty$ solution along different trajectories. Therefore ε represents a singular perturbation to the $\varepsilon = 0$ solutions.

2. We have been assuming so far that the conductivity $\sigma(\phi)$ is a quadratic function of ϕ, but all features of the above results are more general than this implies. For the results to remain valid, it is sufficient for $\sigma(\phi)$ to be continuous and monotonically decreasing on both sides of $\phi = 0$.

3. The existence of boundary layers near the trailing edge has been confirmed in Monte Carlo simulation of the SPBC system, in the single-strip phase. This strenthens our belief that the Langevin equation, despite its crudeness, captures some essence of the physics behind the lattice models.

4. In a phase space analysis of (2.4), we write a three-dimensional vector $\mathbf{y}(u) = (\psi, \psi', \psi'')$ and visualize the solutions as trajectories in phase space. For any given $J > 0$, there are two fixed points at $(\pm(J/\varepsilon)^{1/2}, 0, 0)$. Linearizing about these fixed points, we find that the eigenvalues are precisely those given by (2.8). Thus, for example, they are spirals for $\varepsilon > \varepsilon_c$. We see from Fig. 3 that the possibilities are much richer than those of $\varepsilon = 0$. The linear stabilities of the fixed points for any $J > 0$ are the same. The fact that only $J < \varepsilon\psi_l^2$ gives bounded PBC solutions is apparently due to nonlinear effects, which unfortunately cannot be explained by the behavior in the vicinity of the fixed points. A rigorous proof of the significance of the special value $\varepsilon\psi_l^2$ goes beyond the scope of this paper.

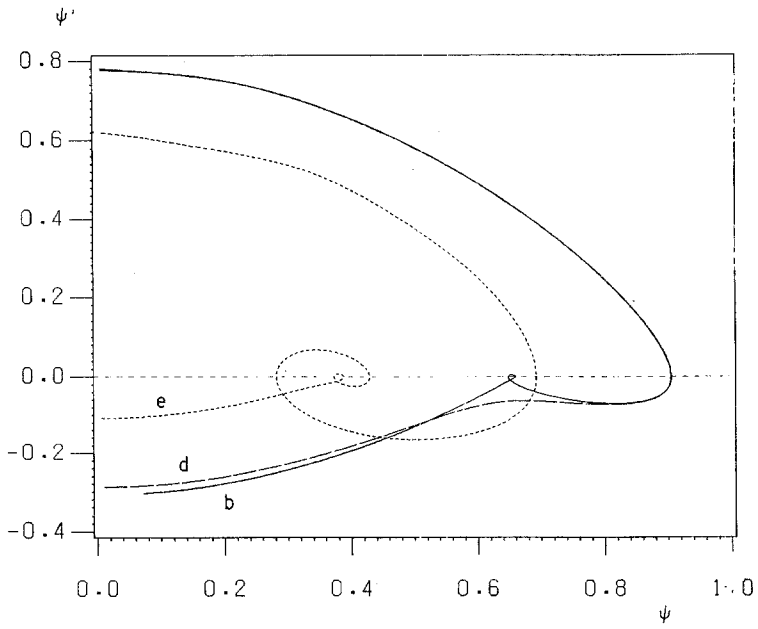

Fig. 3. Projection of the phase-space trajectories of the numerical solutions of Figs. 1b, 1d, and 1e onto the (ψ, ψ') subspace. In cases (b) and (e), the fixed points appear as spirals.

To summarize, the first three features of previous SPBC simulation as mentioned in Section 1 are predicted by the analysis of the continuum model. Now we will focus on the fourth.

3. STABILITY ANALYSIS

Based on the steady-state solutions we found above, the single- to multistrip transformation observed in the SPBC system can be understood in the same framework in which the crystal growth from melts[7] or the hydrodynamic instability of the Saffman–Taylor problem[8] is discussed. Phenomenologically, an initially stable system undergoes an instability as some control parameter is changed. Eventually the system transforms into some new configuration which is globally more stable than the initial one. In each of the above examples, the initial instability is associated with the interfaces, which was first studied systematically by Mullins and Sekerka.[11] Such interfaces separate in general the two bulk phases of a binary system.

To illustrate the analogy claimed above, we will derive in this section the initial interfacial instability of the SPBC system based on our con-

tinuum model of the last section. Consider a particle strip of width $L/2$, tilted at an angle θ with respect to the field E, which points in the $+y$ direction. Because of the tilting (which is *interpreted* as a result of imposing SPBC), there will be a trailing interface and a leading interface. As shown in the last section, boundary layers are associated only with the trailing one, as a result of spatial anisotropy induced by E. Since the two interfaces are far apart, we shall consider each separately.

At low temperature, we are allowed to treate the interface as a contour of negligible thickness ξ, for ξ is much smaller than any other lengths of concern. Under this low-temperature approximation, the bulk equation is reduced to a pair of equations, one for each side of the interface. The interface itself plays the role of a moving boundary at which the bulk solutions have to match. Away from the interfacial region (of thickness ξ), the bulk satisfies diffusion equations supplemented by the driven current:

$$\frac{\partial \phi}{\partial t} = D\nabla^2 \phi + \lambda E_\perp \phi_\alpha \partial_u \phi + \lambda E_{||} \phi_\alpha \partial_v \phi \tag{3.1}$$

where α labels the two bulk phases: $\phi_\alpha = \pm \phi_B$, the constant bulk densities deep in the two phases. $E_\perp \equiv E \sin\theta$ and $E_{||} \equiv E \cos\theta$ are the components perpendicular and parallel to the planar interface. Notice that the diffusion constant D is the same in both phases, due to Ising symmetry. The differences between (3.1) and (2.1) involve higher-order terms in derivatives and in ϕ. They account for the details of the profile of the interfaces of thickness ξ. Such details are irrelevant to our consideration of the interfacial instability.

We first consider the trailing interface. Thus, $\phi(u \to \pm\infty) = \pm\phi_B$, $\phi(u \to 0^\pm) = \pm\phi_I$, where the value at the interface $\phi_I \sim \phi_{\text{eq}} \psi_t$, greater than the value ϕ_B deep in the bulk, is due to the presence of boundary layers. The bulk equations can readily be solved for the steady state $\phi_E(u)$ of a planar interface that lies on the v axis:

$$\phi_E(u) = \phi_\alpha + (\phi_I - \phi_B)\, e^{-|u|/l_\perp} \tag{3.2}$$

The ramps created by the boundary layers decay into the bulk over $l_\perp \equiv (\lambda D^{-1} E_\perp \phi_B)^{-1}$. On the contrary, with the absence of a boundary layer, the solution for the leading interface is just a kink with uniform densities $\pm\phi_B$. Therefore, the combined steady-state solution to (3.1) is precisely the PBC solution of (2.4), with the interfacial regions shrinking to zero under the low-temperature approximation.

The steady state is characterized by nonzero current. The total current is

$$\mathbf{J}^{\text{tot}} = -D\nabla\phi_E(u) - \mathbf{E}\phi_\alpha[\phi_E(u) - \phi_\alpha] + \mathbf{J}^0 \tag{3.3}$$

Deep in the bulk, as $\phi_E \to \pm\phi_B$, the total current becomes uniform at the value $\mathbf{J}^0 \equiv \mathbf{E}\sigma(\phi_B)$. The component of $\mathbf{J}^{\text{tot}}$ perpendicular to the interface, however, is uniform *everywhere*:

$$\begin{aligned} J_\perp^{\text{tot}} &= -D\partial_u \phi_E(u) - E_\perp \phi_\alpha [\phi_E(u) - \phi_\alpha] + J^0 \sin\theta \\ &= J^0 \sin\theta \end{aligned} \tag{3.4}$$

The last equality is a direct consequence of (3.1).

To exhibit interfacial instability, we consider for the planar trailing interface the response to small perturbation:

$$\zeta(v) = \zeta_1 e^{ikv - i\omega t} \tag{3.5}$$

Thus, $u = \zeta(v)$ locates the undulated interface. The sign of $-i\omega$ will then determine the stability. The physical origin of such perturbation is thermal fluctuation, which, though rare at low temperature, is capable of spontaneously generating $\zeta(v)$ in a short time scale compared to the response time of the interface. The undulation inevitably modifies the nearby bulk environment:

$$\begin{aligned} \phi(u) &= \begin{cases} \phi_B + (\phi_I - \phi_B)\, e^{-u/l_\perp} + \phi_1 e^{ikv - i\omega t - pu}, & u > \zeta \\ -\phi_B - (\phi_I - \phi_B)\, e^{u/l_\perp} + \phi_1' e^{ikv - i\omega t + p'u}, & u < \zeta \end{cases} \\ &\approx \begin{cases} \phi_I - (\phi_I - \phi_B)\, u/l_\perp + \phi_1 e^{ikv - i\omega t - pu}, & u > \zeta \\ -\phi_I - (\phi_I - \phi_B)\, u/l_\perp + \phi_1' e^{ikv - i\omega t + p'u}, & u < \zeta \end{cases} \end{aligned} \tag{3.6}$$

The small amplitudes ϕ_1 and ϕ_1' are of the same order as ζ_1. Here $\operatorname{Re} p > 0$ and $\operatorname{Re} p' > 0$.

Because of local conservation, it normally takes a very long time to change the geometry of the interface. In contrast, the density *at* the interface adjusts itself very rapidly to the local environment, for the particles there are most mobile. Such a change is described by the Gibbs–Thomson relation,[12] which serves as a moving boundary condition:

$$\phi(\text{interface}) \mp \phi_I = \Delta\phi_I d_0 \kappa \tag{3.7}$$

where $\Delta\phi_I = 2\phi_I$, d_0 is the capillary length proportional to the surface tension, and $\kappa = -(\delta/\delta\zeta) \int dv [1 + (\partial_v \zeta)^2]^{1/2}$ is the local curvature. Notice that the term on the right accounts solely for the effect of the surface tension minimizing the surface area, while the effect of the field is implicitly contained in the constants $\mp\phi_I$. Although this is an assumption without rigorous justification, it is a plausible and a natural extension of the corresponding equilibrium condition.

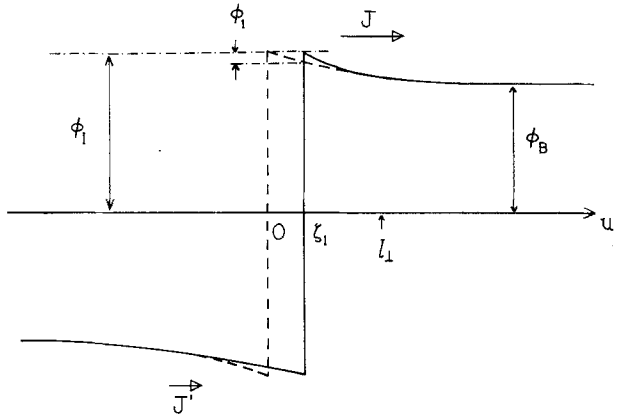

Fig. 4. A planar trailing interface is displaced locally to the right by ζ_1. This induces ϕ_1 and ϕ_1', which in turn create an excess current $J - J'$, forcing the interface to advance further. For simplicity, the case of zero curvature is depicted here.

The undulation creates imbalance of the currents, which results in the motion of the interface:

$$\hat{n} \cdot [\mathbf{J}^{\text{tot}}(\zeta^+) - \mathbf{J}^{\text{tot}}(\zeta^-)] = \Delta\phi_I \frac{\partial \zeta}{\partial t} [1 + (\partial_v \zeta)^2]^{-1/2} \tag{3.8}$$

where the normal is $\hat{n} = (\hat{u} - \hat{v}\partial_v \zeta)[1 + (\partial_v \zeta)^2]^{-1/2}$. The excess of the *transverse* currents is neglected in (3.8), because only the immediate neighborhood of the interface is considered. Away from the interface, excess current is responsible for *bulk* excitations, which are not of concern to the interface. A schematic illustration of (3.5)–(3.8) is depicted in Fig. 2.

Equations (3.1), (3.7), and (3.8) constitute a mathematically complete description of the evolution of the interface. In a linear stability analysis, we need only keep terms up to $O(\zeta_1)$, $O(\phi_1)$, and $O(\phi_1')$. By substituting (3.6) into (3.1), the extent of the bulk undulation, p and p', is determined:

$$\begin{aligned} p^2 - k^2 - p l_\perp^{-1} + ikl_{||}^{-1} - \tilde{\omega} = 0 \\ p'^2 - k^2 - p' l_\perp^{-1} - ikl_{||}^{-1} - \tilde{\omega} = 0 \end{aligned} \tag{3.9}$$

where $l_{||}^{-1} \equiv \lambda D^{-1} E_{||} \phi_B$ and $\tilde{\omega} \equiv -i\omega/D$. Using $\kappa = \partial_v^2 \zeta + O(\zeta^2)$, (3.6) and (3.7) give

$$\phi_1 = \phi_1' = [-\Delta\phi_I d_0 k^2 + (\phi_I - \phi_B) l_\perp^{-1}] \zeta_1 \tag{3.10}$$

Both effects of relaxation by the surface tension and that of amplification

by the ramps are apparent in (3.10). Given these adjustments to the bulk, the interface moves in accord to (3.8):

$$\hat{n}\cdot[(D\nabla\phi_E+\lambda\mathbf{E}\phi_\alpha\phi_E)_{\zeta^-}-(D\nabla\phi_E+\lambda\mathbf{E}\phi_\alpha\phi_E)_{\zeta^+}]=\Delta\phi_I\frac{\partial\zeta}{\partial t}[1+(\partial_v\zeta)^2]^{-1/2} \tag{3.11}$$

Using (3.6), we found for the linear terms

$$\phi_1(p+p')+2l_\perp^{-1}(\phi_I-\phi_B)\,\zeta_1 l_\perp^{-1}-2l_\perp^{-1}\phi_1=-i\omega\Delta\phi_I D^{-1}\zeta_1 \tag{3.12}$$

After eliminating ϕ_1 and ϕ_1' by (3.10), we get

$$\tilde{\omega}=(p+p')\left(\frac{\delta\phi}{\Delta\phi_I}l_\perp^{-1}-d_0k^2\right)+2d_0k^2l^{-1} \tag{3.13a}$$

Here we denote $\phi_I-\phi_B$ by $\delta\phi$, which is of order ε for small ε. By (3.9)

$$p+p'=l_\perp^{-1}+l_\perp^{-1}[(1+4k^2l_\perp^2+4\tilde{\omega}l_\perp^2)^2+(4kl_\perp^2l_{\|}^{-1})^2]^{1/4}\cos\frac{\alpha}{2} \tag{3.13b}$$

with α, in the range from 0 to $\pi/2$, defined by

$$\tan\alpha=\frac{4kl_{\|}^{-1}}{l_\perp^{-2}+4(k^2+\tilde{\omega})} \tag{3.13c}$$

In (3.13a), the physical content of the term proportional to d_0k^2 is pure relaxation, whereas that of those proportional to $l_\perp^{-1}$ is more subtle: their presence implies that the density profile associated with the initial *planar* interface is still influencing the interface at later times. This memory effect originates from the gradient of the bulk density (from ϕ_I to ϕ_B) over a distance $l_\perp$ much greater than ζ_1.

Now it is straightforward to solve for the relaxation or amplification rate $\tilde{\omega}$ from (3.13). First, in the limit $k\to 0$, we find

$$\tilde{\omega}(0)=2\frac{\delta\phi}{\Delta\phi_I}l_\perp^{-2}\left(1+2\frac{\delta\phi}{\Delta\phi_I}\right)>0 \tag{3.14}$$

which clearly displays the instability. Expanding about $k=0$, we find to leading order

$$p+p'=2l_\perp^{-1}[1+l_\perp^2\tilde{\omega}(k)+k^2l_\perp^2+(kl_\perp^2l_{\|}^{-1})^2+\cdots]$$

Hence,

$$\tilde{\omega}(k)=2\frac{\delta\phi}{\Delta\phi_I}l_\perp^{-2}[1+l_\perp^2\tilde{\omega}(k)+k^2l_\perp^2+(kl_\perp^2l_{\|}^{-1})^2+\cdots]$$

which yields

$$\frac{\tilde{\omega}(k)-\tilde{\omega}(0)}{\tilde{\omega}(0)} \approx k^2 l_\perp^2 [1+(l_\perp l_{||}^{-1})^2] + \cdots$$

$$= k^2 l_\perp^2 \left(\frac{1}{\sin^2\theta}\right) + \cdots \tag{3.15}$$

This is valid for $\theta \neq 0$ and small $\delta\phi/\Delta\phi_I$. At large k^2, $\tilde{\omega}(k) \approx -2d_0 k^3 + \cdots$, so that $\tilde{\omega}(k)$ has one zero at some finite k, denoted by k_c. The interface is therefore unstable against small undulation of wavelength longer than k_c^{-1}. Using (3.13), k_c is then determined implicitly by

$$\tilde{\omega}(k_c)\, l_\perp^3\, d_0^{-1} = \left\{1 + [1 + 16(k_c l_\perp)^4 + 8(k_c l_\perp)^2 + 16(k_c l_\perp)^2 \cot^2\theta]^{1/4} \cos\frac{\alpha}{2}\right\}$$

$$\times \left[\frac{\delta\phi}{\Delta\phi_I} l_\perp d_0^{-1} - (k_c l_\perp)^2\right] + 2(k_c l_\perp)^2$$

$$= 0 \tag{3.16}$$

with $k = k_c$ and $\tilde{\omega} = 0$ in the definition of α in (3.13c). For any given $(\delta\phi/\Delta\phi_I)\, l_\perp d_0^{-1}$, k_c can be determined numerically as a function of the angle of tilt θ. Since $D \sim -\lambda r \sim \lambda d_0^{-2}$, $\delta\phi/\Delta\phi_I \sim \varepsilon$ for small ε, and of order unity for large ε, we deduce roughly that $l_\perp^{-1} \sim d_0^{-1}\varepsilon$ and hence $(\delta\phi/\Delta\phi_I)\, l_\perp d_0^{-1} \sim O(1)$ for small ε and of order $1/\varepsilon$ for large ε. Figure 5 gives plots of some typical numerical results. This and the result of $\tilde{\omega}(0)$ show that the instability diminishes as $E \to 0$ or $\theta \to 0$. This is in agreement with simulation for the well-established stability of an interface parallel to the field (i.e, $\theta = 0$).

4. COMPARISON WITH SIMULATION

In connection with simulation, the results here suggest that the single- to multistrip transition is of kinetic nature, rather than of thermodynamic nature like a first-order transition as originally conceived. This assertion is supported by the absence of hysterisis even at such a low temperature as $0.8T_c$ $(E=0)$.[4] Furthermore, between the initial single- and the final multistrip configuration, the system is characterized by fingers of definite width with steady speed of growth (see Fig. 6). The multistrip configuration emerges when fingers grow to wrap around the system. This fingering is similar to those in crystal growth and in the Saffman–Taylor problem. It is of considerable interest to investigate further the kinetics of fingering and to characterize this intermediate "steady state" by the finger parameters.

In order to relate to simulation more quantitatively, we reinterpret our data from SPBC runs as follows. For small shift h, the length $L_{||}$ along the interface in the single-strip phase plays the role of the maximum wavelength k^{-1} above:

$$L_{||} \equiv (L_y^2 + h^2)^{1/2}$$

Accordingly, for a given $\theta = \sin^{-1}(h/L_{||})$, the single strip will become unstable when $L_{||}$ exceeds a critical length $L_c(\theta) \equiv 2\pi k_c(\theta)^{-1}$. Since the interstep distance d_{step} is $L_y/h = \cot\theta$, this implies, for a given $L_{||}$, an instability for sufficiently large number of steps h or small d_{step}. Therefore, for a given θ, there is a unique L_c below which the system is in a single-strip phase, and above which in a multistrip phase. Using the data of ref. 4 and new runs for systems $(L_x \times L_y)$ 24×24, 60×60, and 60×312,[2] which go multistrip at $h = h_c = 5$, 8, and 23, respectively, we plot $L_c(\theta)^{-1}$ versus $\sin\theta$ in Fig. 7. The curving toward the origin, set in by the $L_y = 312$ data point, is consistent qualitatively with our stability analysis (Fig. 5); in particular, the disappearance of single-strip phase for any finite θ in the thermodynamic limit is suggested. Unfortunately, as seen from the vertical

[2] Test runs on a 24×100 system show that h_c is insensitive to the lateral size L_x.

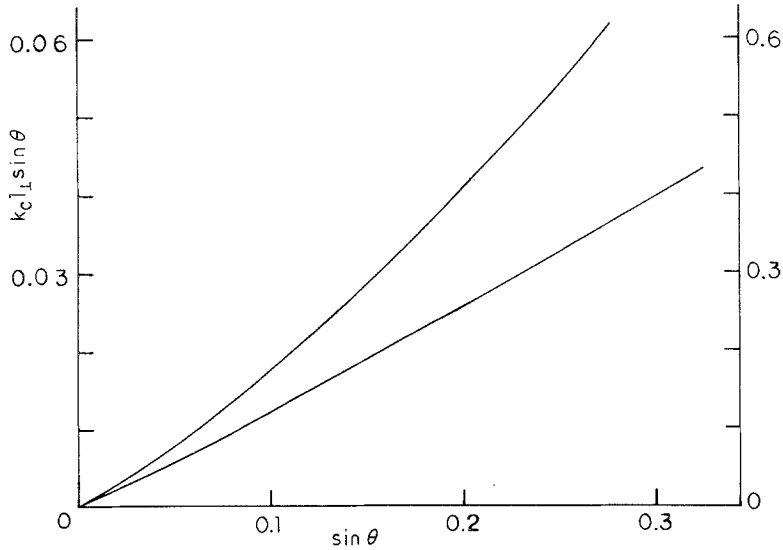

Fig. 5. Numerical results fom (3.16) of the critical wavenumber $k_c(\theta)\, l_\perp \sin\theta \sim k_c d_0^2 / E\phi_B$ versus the angle of tilt, for the dimensionless parameter $(\delta\phi/\Delta\phi_I)\, l_\perp d_0^{-1} = 0.01$ on the right, and 1 on the left.

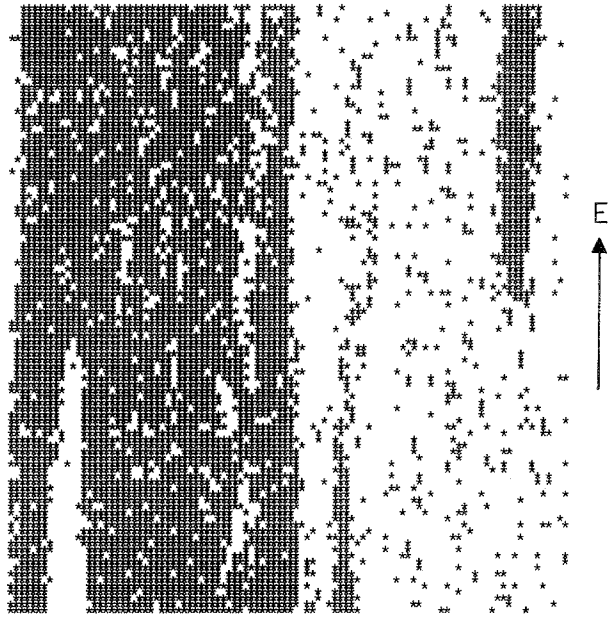

Fig. 6. A snapshot of an SPBC 100×100 configuration from simulation, during its evolution from a single strip (originally tilted to the left) to multistrips. The vertical boundaries are joined by PBC, whereas the horizontal ones are relatively shifted by $h_c = 12$ before joining. The particle and the hole finger grow steadily until they wrap around the system to form a multistrip configuration. Though the leading edge is very noisy, it remains stable throughout.

scale of Fig. 7, to explore this asymptotic behavior demands enormous computational effort.

Although the stability analysis suggests a mechanism for the initial growth of fingers, there are important differences between the continuum and the lattice model. In ref. 4, we emphasized the subtle interplay among the field E, boundary conditions, and the lattice. Here in the continuum model, lattice anisotropy is neglected. Ultimately, a complete theory must also account for the lattice which governs the selection process, as seen in the direction of fingering and the subsequent orientation of the multistrip. Also, screening is very pronounced; eventually only one finger is seen to grow along a narrow channel of width h.

In simulations, the multistrip phase is also unstable with increasing tilt. It undergoes a series of n-strip to $(n-1)$-strip merging transitions, where *at* the transition the interface in the $(n-1)$-strip phase is always less inclined with respect to E than in the n-strip phase (see ref. 4 for more details). It is tempting to invoke the above splitting mechanism of a single strip in explaining this. Although this may be correct qualitatively, we cau-

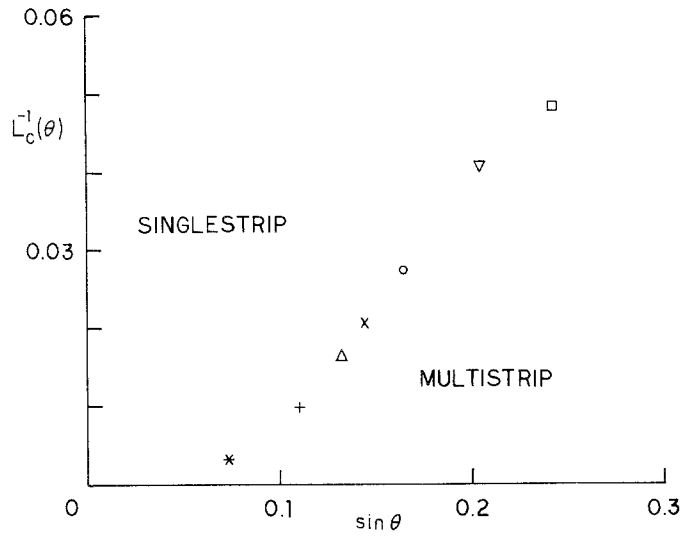

Fig. 7. Simulation results of SPBC runs (from right to left): $L_y = 20$, 24, 36, 48, 60, 100, and 312. Stability analysis predicts the curve to bend toward the origin (cf. Fig. 5).

tion against it, because in the multistrip phase, the spacing between interfaces is fairly small in all the cases we studied. This is true even for systems of large L, as the strip width $w_s \sim L/n \sim L\theta_c$ is consistently small, since the angle of tilt at transition θ_c decreases with increasing L. From the numerical solutions, we knew that for small period the hump appears to be a gradient across the whole strip [see cases (c) and (d) in Fig. 1]. Therefore, in the multistrip phase, neighboring strips are strongly interacting. This is where the above theory breaks down.

5. DISCUSSION AND CONCLUSION

First, we remark on the role of thermal fluctuations that is responsible for the undulation. Since our analysis is based on a low-temperature approximation, such fluctuations are small in amplitude and rare in occurrence. The rarity of such events, however, does not imply that they are slow. In fact, as observed in simulation, disturbance of a planar interface usually occurs in a short time compared to its subsequent relaxation or amplification. Yet, in contrast, they play a negligible role in relaxing or amplifying the disturbance, for otherwise they have to act either in the same or the opposite direction in phase space as of the creation, which is extremely unlikely. This is the justification of dropping the noise term in (2.1) and putting in the undulation by hand in (3.5) and (3.6).

Second, we notice important differences between an interface in steady state and one in equilibrium. The first deals with the Gibbs–Thomson relation (3.7) that fixes the values of the bulk density at both sides of the interface after small disturbance. For simplicity, consider zero surface tension. In equilibrium, the values are determined by the coexistence curve at the given temperature, i.e., $\phi(\text{interface}) = \pm\phi_{eq}(T)$. This ability of local adjustment by the system to the global average density stems from the existence of a free energy. To minimize the free energy, the system tries to pick ϕ_{eq} as the density everywhere, except, of course, right at the interface. On the contrary, a system in steady state does not have a free energy as a guide. Although the density deep in the bulk is similarly determined by the coexistence curve, that at the interface is rather fixed by maintaining a uniform current, a requirement with no equilibrium counterpart.[3] Since this does not operate locally, it would not be easy to argue that ϕ(interface) instantaneously adjusts itself to ϕ_I during its course of evolution. Being aware of this potential pitfall of (3.7), we remark that in order to realize the Mullins–Sekerka instability, the exact value of ϕ(interface) is not crucial. First, it is reasonable to assume, at least for small distortion ζ_1, that $\phi(\zeta^-) = -\phi(\zeta^+)$, since this is just Ising symmetry obeyed by the *local* density function in the Langevin equation. Then it is easy to convince oneself, say, graphically (cf. Fig. 2), that within a reasonable range of value chosen for ϕ(interface), the excess of current so created still yields an unstable planar interface.

At a less conceptual but more technical level, we address the possibility of new kinetic terms introduced by the field. It is appreciated[7] on physical grounds that a moving interface should induce, in the density across the interface, a discontinuity in the form of an (anisotropic) term proportional to the growth velocity on the right-hand side of (3.7), thereby pulling the system away from local equilibrium. Within the linear stability analysis, such a term is expected to be negligibly small, and has been neglected above as well as in other studies.[12,14,15] However, it may be important in the nonlinear regime where the planar interface is substantially distorted.

The most essential feature of this study is the existence of boundary layers. Without the ramps created by such layers, the length $l_\perp$ would be infinite, and the interface would always be stable. This is precisely the case in the equilibrium system,[12,13] in the case of parallel interface (to E), or in a previous study where only antiperiodic configurations were considered[2] (which picks out only tanh-like profiles as discussed in Section 2).

[3] Thus, we have to solve for the steady state from the kinetic equation (Section 2), as opposed to locating the minimum of some functional like $\mathcal{H}\{\phi\}$ in equilibrium.

Our interest in considering the *pair* of interfaces under PBC, besides *one* under *anti*-PBC, is motivated by the first realization of driven *tilted* interfaces and the subsequent transition from single- to multistrip configuration. The current work, on the one hand, provides a plausible framework for understanding the mechanism of the *onset* of such a transition. On the other hand, this represents a simple example of steady-state interfacial instability which is accessible not only to simulation, but also to experiment. It is analogous to the symmetric model introduced by Langer and Turski,[12] where their asymptotic density gradient (due to undercooling which is absent here) plays the role of our field. A similar situation is also encountered in interfacial growth in the presence of a perpendicular field.[14] The ramps also dictate the instability that results from quenching deeper into the ordered phase in nondriven systems,[15] though their physical origin is again different.

ACKNOWLEDGMENTS

The author has benefited from discussions and related collaborations with R. K. P. Zia, G. A. Hagedorn and B. Schmittmann, and he thanks them. He also thanks J. L. Vallés for providing Fig. 6. He is indebted to K. K. Mon and D. P. Landau of the Center for Simulational Physics at the University of Georgia for providing computer time. This work was supported by the NSF through the Division of Materials Research under grant DMR-8817653.

REFERENCES

1. S. Katz, J. L. Lebowitz, and H. Spohn, *Phys. Rev. B* **28**:1655 (1983); *J. Stat. Phys.* **34**:497 (1984); H. van Beijeren and L. S. Schulman, *Phys. Rev. Lett.* **53**:806 (1984).
2. K.-T. Leung, *J. Stat. Phys.* **50**:405 (1988); A. Hernández-Machado and D. Jasnow, *Phys. Rev. A* **37**:626 (1988); A. Hernández-Machado, H. Guo, J. L. Mozos, and D. Jasnow, preprint (1989).
3. K.-T. Leung, K. K. Mon, J. L. Vallés, and R. K. P. Zia, *Phys. Rev. Lett.* **61**:1744 (1988); *Phys. Rev. B* **39**:9312 (1989).
4. J. L. Vallés, K.-T. Leung, and R. K. P. Zia, *J. Stat. Phys.* **56**:43 (1989).
5. H. van Beijeren, R. Kutner, and H. Spohn, *Phys. Rev. Lett.* **54**:2026 (1985).
6. K.-T. Leung and J. L. Cardy, *J. Stat. Phys.* **44**:567 (1986); H. K. Janssen and B. Schmittmann, *Z. Phys. B* **64**:503 (1986); K. Gawadzki and A. Kupiainen, *Nucl. Phys. B* **269**:45 (1986).
7. J. S. Langer, in *Chance and Matter* (Les Houches XLVI 1986), J. Souleti, J. Anninemus, and R. Stora, eds. (Elsevier, 1987); D. A. Kessler, J. Koplik, and H. Levine, *Adv. Phys.* **37**:255 (1988).
8. P. G. Saffman and G. I. Taylor, *Proc. R Soc. Lond. A* **254**:312 (1958); D. Bensimon, L. P. Kadanoff, S. Liang, B. I. Shraiman, and C. Tang, *Rev. Mod. Phys.* **58**:977 (1986).
9. P. C. Hohenberg and B. I. Halperin, *Rev. Mod. Phys.* **49**:435 (1977).

10. G. A. Hagedorn and R. K. P. Zia, private communication.
11. W. W. Mullins and R. F. Sekerka, *J. Appl. Phys.* **34**:323 (1963); **35**:444 (1964); R. F. Sekerka, in *Crystal Growth, an Introduction*, P. Hartman, ed. (North-Holland, Amsterdam, 1973).
12. J. S. Langer and L. A. Turski, *Acta Met.* **25**:1113 (1977).
13. D. Jasnow and R. K. P. Zia, *Phys. Rev. A* **36**:2243 (1987); R. K. P. Zia, R. Bausch, H. K. Janssen, and V. Dohm, *Mod. Phys. Lett. B* **2**:961 (1988).
14. H. Guo and D. Jasnow, *Phys. Rev. A* **34**:5027 (1986); D. Jasnow, in *Far From Equilibrium Phase Transitions*, L. Garrido, ed. (Springer-Verlag, New York, 1988).
15. D. Jasnow, D. A. Nicole, and T. Ohta, *Phys. Rev. A* **23**:3192 (1981); A. Onuki, K. Sekimoto, and D. Jasnow, *Prog. Theor. Phys.* **74**:685 (1985).